JOURNAL OF NATURAL PRODUCTS

Article

Cite This: J. Nat. Prod. 2018, 81, 1343−1356

pubs.acs.org/jnp

Dehydrodiconiferyl Alcohol Inhibits Osteoclast Differentiation and Ovariectomy-Induced Bone Loss through Acting as an Estrogen Receptor Agonist

Wonwoo Lee,[†,‡] Kyeong Ryang Ko,[†,‡] Hyun-keun Kim,[†] Doo Suk Lee,[‡] In-Jeong Nam,[‡] Seonung Lim,[†] and Sunyoung Kim*[,†,‡]

[†]Department of Biological Sciences, Seoul National University, Seoul 151-742, Korea

[‡]ViroMed Co., Ltd., Seoul 151-747, Korea

Supporting Information

ABSTRACT: Estrogen deficiency after menopause increases bone loss by activating RANKL-induced osteoclast differentiation. Dehydrodiconiferyl alcohol (DHCA), a lignan originally isolated from *Cucurbita moschata*, has been thought to be a phytoestrogen based on its structure. In this study, we tested whether DHCA could affect RANKL-induced osteoclastogenesis *in vitro* and ovariectomy-induced bone loss *in vivo*. In RAW264.7 cells, DHCA inhibited RANKL-induced differentiation of osteoclasts. Consistently, expression of the six osteoclastogenic genes induced by RANKL was down-regulated. DHCA was also shown to suppress the NF-κB and p38 MAPK signaling pathways by activating AMPK. Data from transient transfection assays suggested that DHCA might activate the estrogen receptor signaling pathway. Effects of DHCA on RANKL-induced osteoclastogenesis were reduced when cells were treated with specific siRNA to ERα, but not to ERβ. Interestingly, DHCA was predicted from molecular docking simulation to bind to both ERα and ERβ. Indeed, data from an estrogen receptor competition assay revealed that DHCA acted as an agonist on both estrogen receptors. In the ovariectomized (Ovx) mouse model, DHCA prevented Ovx-induced bone loss by inhibiting osteoclastogenesis. Taken together, our results suggest that DHCA may be developed as an efficient therapeutic for osteoporosis by regulating osteoclastogenesis through its estrogenic effects.

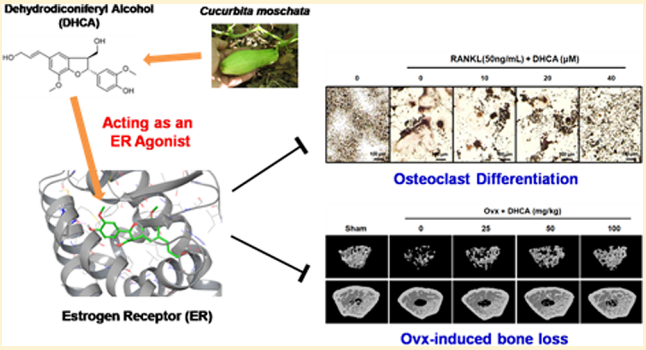

Osteoporosis is a skeletal disease characterized by a reduced density and quality of bones, leading to increased susceptibility to fractures.[1,2] Osteoporosis has become a serious health problem due to its prevalence.[3] Currently, more than 200 million people are estimated to suffer from this disease worldwide,[4] with the number of patients expected to grow rapidly with the rise in the elderly population.[5] There are several FDA-approved drugs available for osteoporosis such as denosumab,[6] ibandronate,[7] and raloxifene.[8] However, because of limitations of their efficacy and safety, there is still a huge unmet medical need for a solution to this degenerative disease.

Excessive bone resorption is a major step in the pathogenesis of osteoporosis,[9] and osteoclasts are responsible for this process by degrading the bone matrix.[10] Several signaling molecules involved in osteoclastogenesis, the differentiation of osteoclasts from precursor cells, have been implicated as a promising target for the prevention or treatment of osteoporosis. Interaction of RANKL [receptor activator of nuclear factor kappa-B (NF-κB) ligand] with its receptor, RANK, initiates osteoclast differentiation by activating various signaling pathways, such as those involving NF-κB[11] and mitogen-activated protein kinases (MAPKs).[12] NFATc1 (nuclear factor of activated T cells, cytoplasmic, calcineurin dependent 1), a downstream transcription factor in NF-κB[13] and MAPKs[13,14] pathways, plays a master role in the regulation of various genes involved in osteoclast functions,[15] such as MMP-9 (matrix metalloproteinase-9), DC-STAMP (dendrocyte expressed seven transmembrane protein), and cathepsin K. In experiments involving AMPK-knockout mice, the AMPK (AMP-activated protein kinase) signaling pathway has also been shown to play a key role in osteoclastogenesis by preventing bone loss.[16]

It is established that estrogen deficiency during menopause generates significant bone loss.[9] Estrogen can suppress bone resorption by directly inhibiting RANKL-induced osteoclastogenesis through the control of c-Jun activity.[17] Many studies also revealed that estrogen could regulate osteoclastogenesis by down-regulating the production of TNF-α, IL-1β, and IL-6, resulting in the enhanced production of RANKL and M-CSF in stromal cells.[18] Such effects of estrogen on the prevention of bone loss are strongly supported by data from experiments involving knockout mice lacking estrogen receptor alpha

Received: November 3, 2017
Published: June 5, 2018

DOI: 10.1021/acs.jnatprod.7b00927
J. Nat. Prod. 2018, 81, 1343−1356

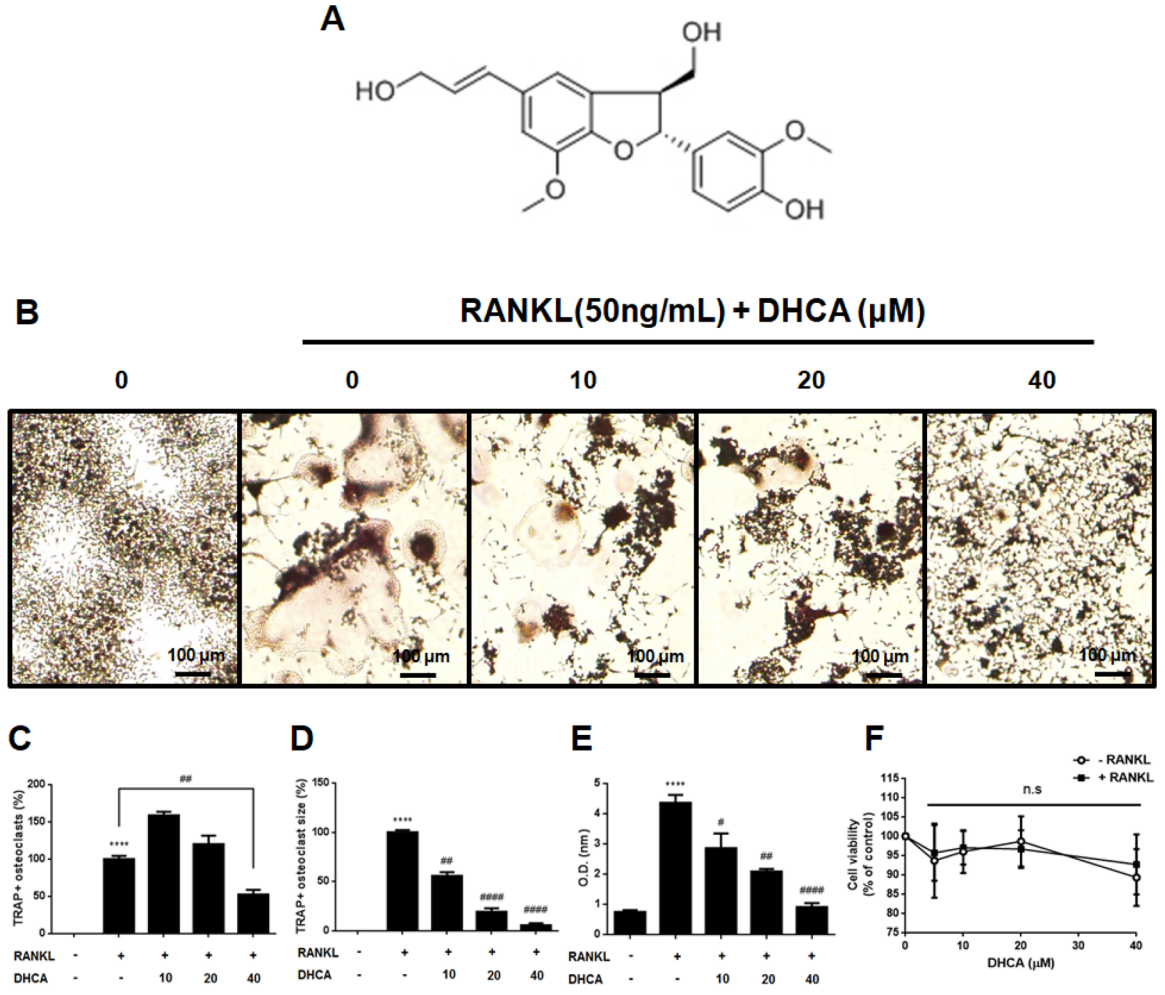

Figure 1. DHCA suppressed RANKL-induced osteoclast differentiation. (A) Chemical structure of DHCA. (B) TRAP-positive multinucleated cells were visualized by TRAP staining. (C) The number of TRAP-positive multinucleated cells were counted under the microscope. (D) The size of TRAP-positive multinucleated cells was measured under the microscope. (E) TRAP activity was measured at 450 nm followed by a TRAP activity assay. RAW264.7 cells were treated with RANKL (50 ng/mL) and cultured in the presence of DHCA for 5 days. (F) RAW264.7 cells were treated with or without RANKL and various concentrations of DHCA for 72 h. Cells were then subjected to MTT assay as described in the Experimental Section. Values represent the mean ± SEM of three independent experiments. ****$p < 0.0001$ compared with control; $^{\#}p < 0.05$, $^{\#\#}p < 0.01$, $^{\#\#\#\#}p < 0.0001$ compared with that treated with RANKL alone.

(ERα).[19] Consequently, a variety of phytoestrogens and selective estrogen receptor modulators (SERMs) have been tested for their possible use in treating postmenopausal osteoporosis.[20]

Dehydrodiconiferyl alcohol (DHCA) is a lignan isolated from water-soluble extracts of *Cucurbita moschata*.[21] DHCA had been thought to be a member of the phytoestrogen family. Indeed, our group previously reported that synthetic DHCA contains a wide range of estrogen-like activities with effects such as anti-adipogenic,[21] anti-inflammatory,[22] and anti-oxidative effects[23] by regulating C/EBPβ, NF-κB, and AMPK signaling pathways, respectively. In this study, we hypothesized that DHCA might have a beneficial effect(s) on preventing osteoclastic bone loss by acting as an estrogen receptor agonist. The effects of DHCA on RANKL-induced osteoclastogenesis *in vitro* and on ovariectomy-induced bone loss *in vivo* have been investigated, and the underlying mechanisms also have been studied.

RESULTS AND DISCUSSION

DHCA Inhibits RANKL-Induced Osteoclast Differentiation of RAW264.7 Cells with No Cytotoxic Effect. RAW264.7 cells are the murine preosteoclast cell line that can differentiate into osteoclasts when stimulated with RANKL.[17] TRAP (tartrate-resistant acid phosphatase) is a specific marker for mature osteoclasts.[24] To induce osteoclastogenesis, RAW264.7 cells were treated with RANKL (50 ng/mL) and various concentrations of DHCA (10, 20, or 40 μM) for 5 days. TRAP-positive multinucleated cells were counted, and TRAP activity was measured. As shown in Figure 1B–D, DHCA treatment reduced the number and size of TRAP-positive multinucleated cells in a dose-dependent manner. Consistently, TRAP activity was also decreased by DHCA in a similar way (Figure 1E).

To investigate the effects of DHCA on bone resorption activity, the pit formation assay was performed. RAW264.7 cells were seeded on an osteoassay plate and cotreated with RANKL and various concentrations of DHCA for 5 days. As shown in Supplementary Figure 1, DHCA treatment inhibited RANKL-induced bone resorption in a dose-dependent manner.

Effects of DHCA on cell viability were measured. RAW264.7 cells were cultured with or without RANKL in the presence of DHCA, and cell viability was examined by MTT assay. As shown in Figure 1F, DHCA had little effect on cell viability at all

DOI: 10.1021/acs.jnatprod.7b00927
J. Nat. Prod. 2018, 81, 1343−1356

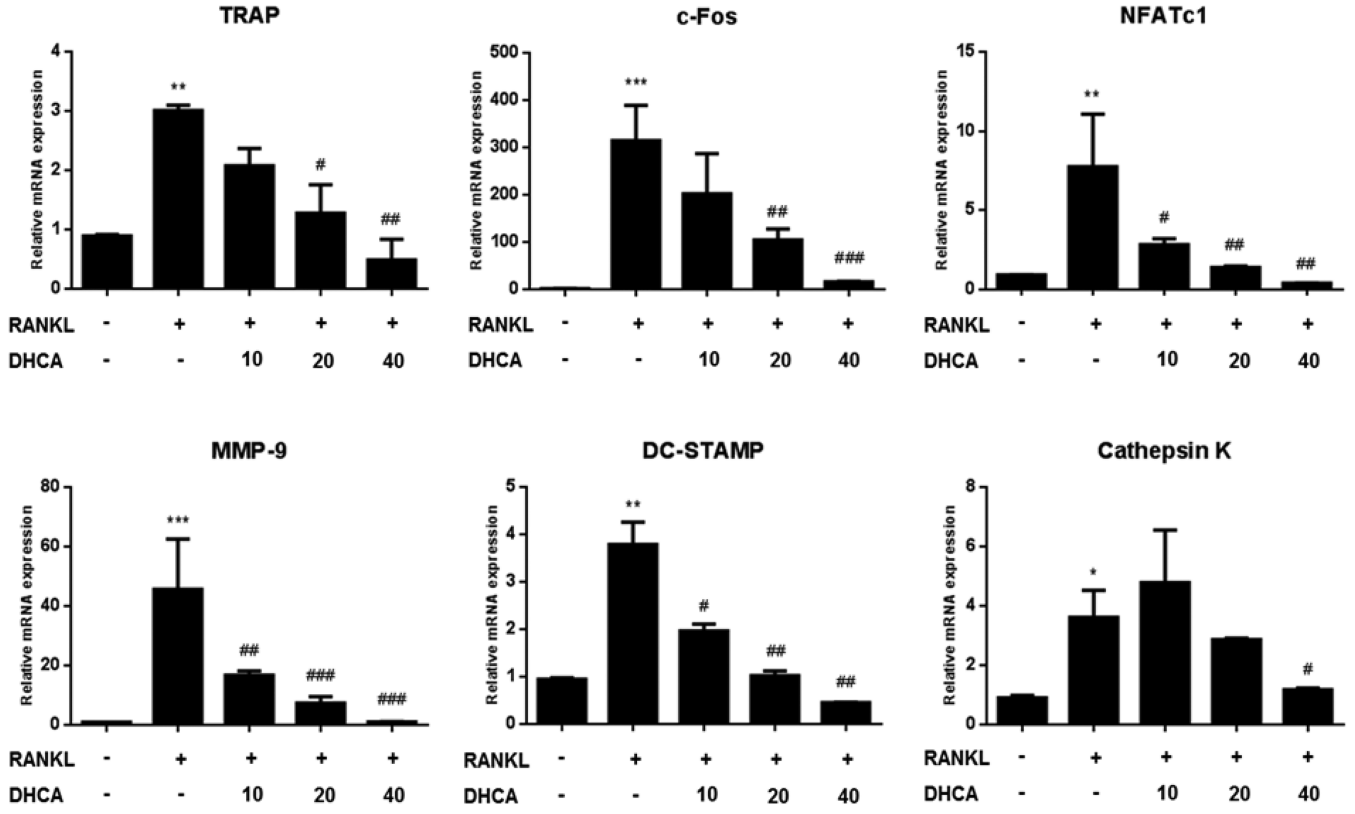

Figure 2. DHCA inhibited osteoclastogenic gene expression during RANKL-induced osteoclastogenesis. Total RNAs were prepared followed by quantitative RT-PCR using specific primers for TRAP, c-Fos, NFATc1, MMP-9, DC-STAMP, and cathepsin K. RAW264.7 cells were treated with RANKL (50 ng/mL) and cultured in the presence of DHCA for 24 h. Values represent the mean ± SEM of three independent experiments. $^{*}p < 0.05$, $^{**}p < 0.01$, $^{***}p < 0.001$ compared with control; $^{\#}p < 0.05$, $^{\#\#}p < 0.01$, $^{\#\#\#}p < 0.001$ compared with that treated with RANKL alone.

concentrations. DHCA did not have any cytotoxic effects during 72 h regardless of the presence of RANKL.

DHCA Inhibits the Expression of Osteoclastogenic Genes. NFATc1 is a well-known transcription factor playing a major role in osteoclastogenesis. RANKL stimulation to preosteoclasts increases expression of NFATc1, leading to the activation of various osteoclastogenic genes involved in differentiation and functions of osteoclasts such as TRAP, c-Fos, DC-STAMP, MMP-9, and cathepsin K.[25,26] To test the effects of DHCA on these genes, RAW264.7 cells were cocultured with RANKL and DHCA for 24 h, and the RNA level was measured by quantitative RT-PCR. DHCA treatment decreased the RNA level of NFATc1 and c-Fos, along with other osteoclast-specific genes such as TRAP, MMP-9, DC-STAMP, and cathepsin K, in a concentration-dependent manner (Figure 2).

DHCA Suppresses RANKL-Induced NFATc1 and c-Fos Production via NF-κB and p38 MAPK inhibition. During RANKL-induced osteoclastogenesis, NFATc1 and c-Fos have been known to be activated by NF-κB and MAPK signaling pathways, which are critical steps in the differentiation of osteoclasts.[27,28] To test the effects of DHCA on the RANKL-induced protein expression of transcription factors, RAW264.7 cells were cotreated with RANKL and DHCA for 24 h, and the protein levels of NFATc1 and c-Fos were measured by Western blot. As shown in Figure 3A, DHCA treatment inhibited RANKL-induced production of NFATc1 and c-Fos in a concentration-dependent manner.

Next, it was tested whether DHCA could also suppress the RANKL-induced nuclear translocation of NFATc1. RAW264.7 cells were cocultured with RANKL and various concentrations of DHCA for 24 h, and the nuclear proteins were isolated followed by Western blot analysis. RANKL treatment increased NFATc1 translocation into the nucleus, but DHCA reduced it in a dose-dependent manner (Figure 3B).

To further investigate the effects of DHCA on the RANKL-induced signaling pathway, RAW264.7 cells were cotreated with RANKL and DHCA for 30 min, and the phosphorylation status of Akt-IKK and MAPKs was determined by Western blot. When cells were treated with RANKL, Akt was efficiently phosphorylated, but its level was highly decreased by DHCA treatment (Figure 3C). It was also found that phosphorylation of IKK, which is downstream of Akt, was suppressed in the presence of DHCA (Figure 3C). Consistent with these results, RANKL-induced degradation of the IκB proteins was recovered by DHCA (Figure 3C). These data indicated that DHCA might effectively control the Akt-IKK-NF-κB axis activated by RANKL.

The phosphorylation status of MAPKs was also affected by DHCA. RANKL stimulation increased phosphorylation of JNK, p38, and ERK (Figure 3D), and DHCA treatment decreased p38 phosphorylation, but did not affect either JNK or ERK (Figure 3D). Taken together, DHCA negatively controlled the RANKL signaling pathway by inhibiting the Akt-IKK-NF-κB axis and the p38 MAPK.

DHCA Attenuated RANKL-Induced Osteoclastogenesis by Activating AMPK. It has been previously reported that AMPK acts as a negative regulator of RANKL-induced osteoclastogenesis, via inactivation of various downstream signaling elements such as p38, JNK, NF-κB, Akt, CREB, c-Fos, and NFATc1.[16,29] Therefore, the effect of DHCA was investigated on AMPK. When RAW264.7 cells were treated with

DOI: 10.1021/acs.jnatprod.7b00927
J. Nat. Prod. 2018, 81, 1343−1356

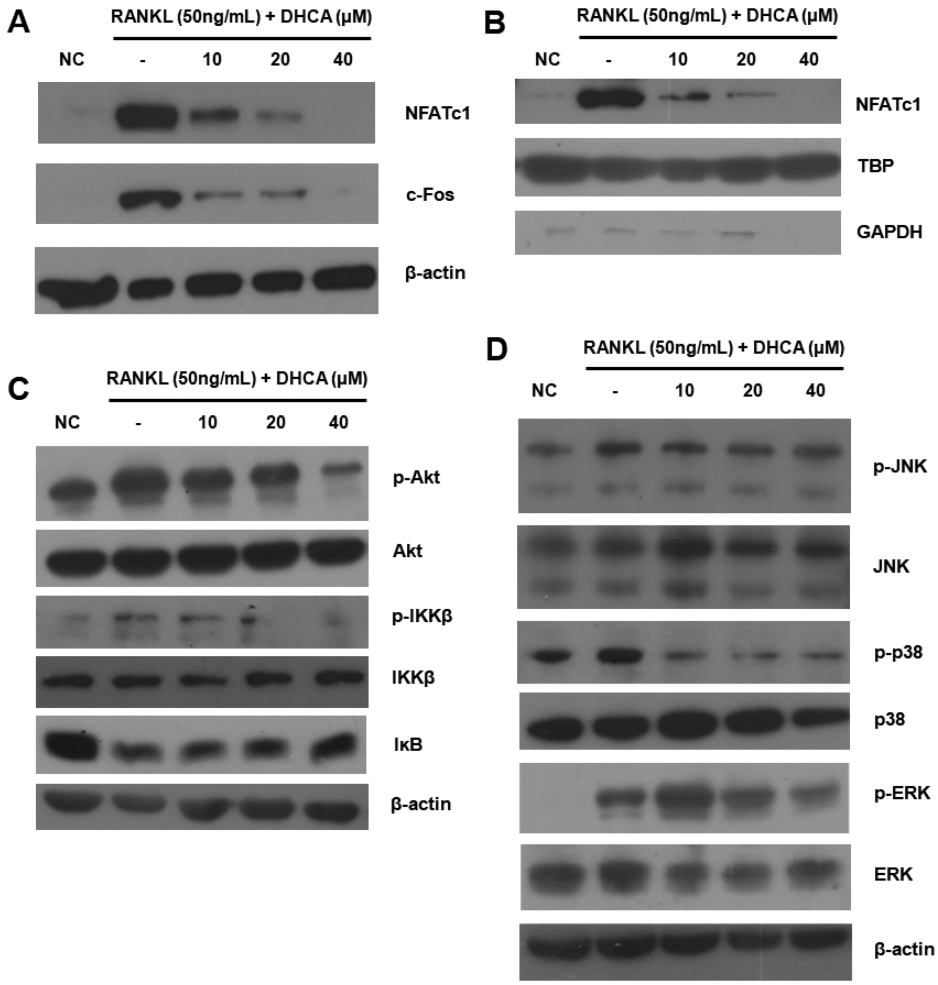

Figure 3. Effects of DHCA on NF-κB and MAPK signaling pathways. (A) Effects of DHCA on the protein level of osteoclastogenic transcription factors. (B) Effects of DHCA on the nuclear translocation of NFATc1. (C) Effects of DHCA on NF-κB signaling pathway. (D) Effects of DHCA on MAPK signaling pathway. RAW264.7 cells were treated with RANKL (50 ng/mL) and cultured in the presence of DHCA for 24 h or 30 min. Total or nuclear proteins were prepared followed by Western blot using antibodies specific for respective proteins.

RANKL alone, the level of phosphorylated AMPK was increased, and this effect was further enhanced upon DHCA treatment (Figure 4A, compare lanes 2 and 5).

To confirm the relationship between AMPK and DHCA, RAW264.7 cells were transfected with siRNA against AMPKα1 followed by treatment with RANKL and DHCA. As shown in Figure 4C−F, the anti-osteoclastogenic effects of DHCA were suppressed when cells were transfected with siRNA. Similarly, the DHCA-mediated reductions of TRAP, NFATc1, and c-Fos expressions were also inhibited by siRNA (Figure 4G). These data indicated that DHCA might suppress osteoclastogenesis by activating AMPK.

Effects of DHCA on Activating AMPK Were Mediated by the Estrogen Signaling Pathway. A significant number of phytochemicals are known to interact with estrogen receptors and act as SERMs.[30] Furthermore, estradiol demonstrates anti-osteoclastogenic activity via activation of AMPK.[17] To investigate the possible mechanisms by which DHCA activates AMPK, an inhibitor assay targeting the upstream factors of AMPK was performed. RAW264.7 cells were cotreated with RANKL, DHCA, and various concentrations of AMPK-upstream inhibitors for 5 days, and TRAP activity was measured. As shown in Figure 5A−C, PKA inhibitor H89 (1−10 μM) and CaMKKβ inhibitor STO609 (1−10 μM) did not interfere with DHCA activity, while the estrogen receptor antagonist fulvestrant (1−10 μM) diminished the effects of DHCA. Furthermore, the level of phosphorylated AMPK was decreased when fulvestrant was cotreated with DHCA, but H89 and STO609 did not alter the level of phosphorylated AMPK (Figure 5D). Consistently, DHCA did not affect the phosphorylation status of PKA and CaMKKβ (Supplementary Figure 2). Therefore, the effects of DHCA on AMPK activation appeared to be mediated by the estrogen receptor, not PKA or CaMKKβ.

To test the effects of DHCA on the estrogen-induced signaling pathway, RAW264.7 cells were transfected with a luciferase reporter plasmid containing nucleotide sequences for estrogen responsive element (ERE). Twenty-four hours later, transfected cells were treated with estradiol or DHCA for 6 h. Total proteins were extracted, and relative luciferase units were measured by luminometer. When cells were treated with DHCA, the level of luciferase activity was increased by DHCA in a concentration-dependent manner (Figure 5E).

Anti-osteoclastogenic Effects of DHCA Were Mediated by ERα, but Not ERβ. There are two different forms of the estrogen receptor, usually referred to as ERα and ERβ, and they are known to regulate osteoclastogenesis differently.[19,31] To investigate which of the two estrogen receptors DHCA interacts with and exerts its effects, antagonists that target the specific

DOI: 10.1021/acs.jnatprod.7b00927
J. Nat. Prod. 2018, 81, 1343−1356

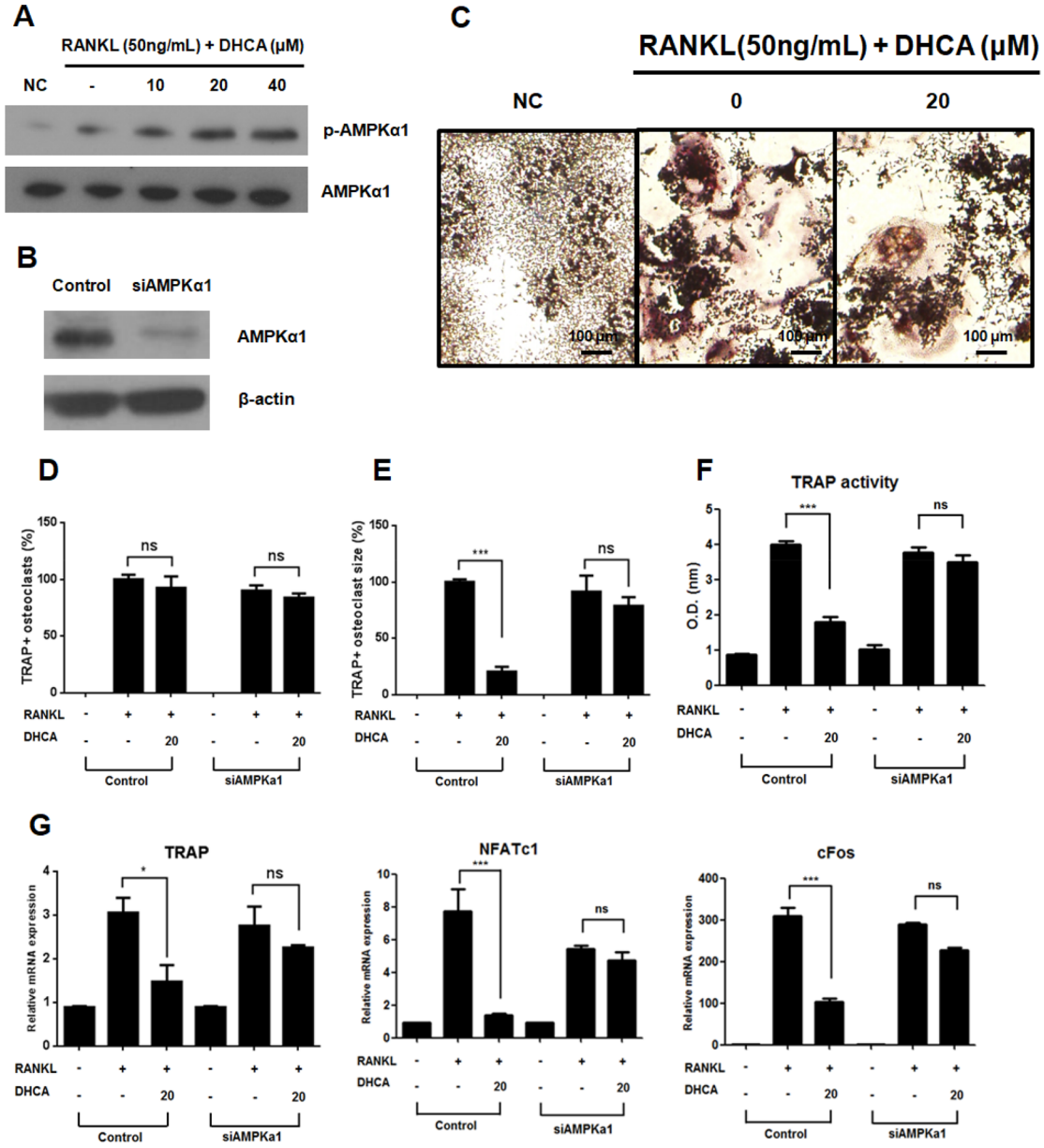

Figure 4. AMPK played a key role in the inhibition of RANKL-induced osteoclast differentiation by DHCA. (A) Phosphorylation status of AMPKα1 was enhanced by DHCA during RANKL-induced osteoclast differentiation. RAW264.7 cells were treated with RANKL (50 ng/mL) and cultured in the presence of DHCA for 24 h. Total protein were prepared followed by Western blot using antibodies specific for respective proteins. (B) The protein level of AMPKa1 was determined by Western blot. (C) TRAP-positive multinucleated cells were visualized by TRAP staining. (D) The number of TRAP-positive multinucleated cells was counted under the microscope. (E) The size of TRAP-positive multinucleated cells was measured under the microscope. (F) TRAP activity was measured, after 5 days, at 450 nm followed by a TRAP activity assay. (G) The expression level of osteoclastogenic genes was measured by quantitative RT-PCR after 24 h. RAW264.7 cells were transfected with AMPKα1 siRNA or control siRNA and then were cotreated with RANKL (50 ng/mL) and DHCA (20 μM). TRAP-stain results with control siRNA transfection are shown in Supplementary Figure 3. Values represent the mean ± SEM of three independent experiments. *$p < 0.05$, ***$p < 0.001$.

estrogen receptor were used. RAW264.7 cells were treated with various concentrations of ERα-specific antagonist MPP (0.1−1 μM) or ERβ-specific antagonist PHTPP (1−10 μM) in the presence of RANKL and DHCA; then RANKL-induced osteoclastogenesis and osteoclastogenic gene expression were measured. As shown in Figure 6A−E, MPP abolished DHCA-mediated inhibition of osteoclastogenesis and expression of osteoclastogenic transcription factor, while PHTPP had no effect.

To confirm the relationship between estrogen receptors and DHCA, RAW264.7 cells were transfected with siRNA against ERα or ERβ followed by treatment with RANKL and DHCA. Anti-osteoclastogenic effects of DHCA were suppressed when cells were transfected with ERα siRNA (Figure 6G−K), whereas these effects were not affected by transfection with ERβ siRNA (Supplementary Figure 4A−F). Taken together, these data indicated that DHCA might interact with ERα, but not ERβ, to inhibit RANKL-induced osteoclast differentiation.

DHCA Was Predicted to Bind with ERα and ERβ by Molecular Docking Simulation. Our data from Figure 6 suggested that DHCA may bind with estrogen receptor, ERα. To study this possibility, a molecular docking simulation was

DOI: 10.1021/acs.jnatprod.7b00927
J. Nat. Prod. 2018, 81, 1343−1356

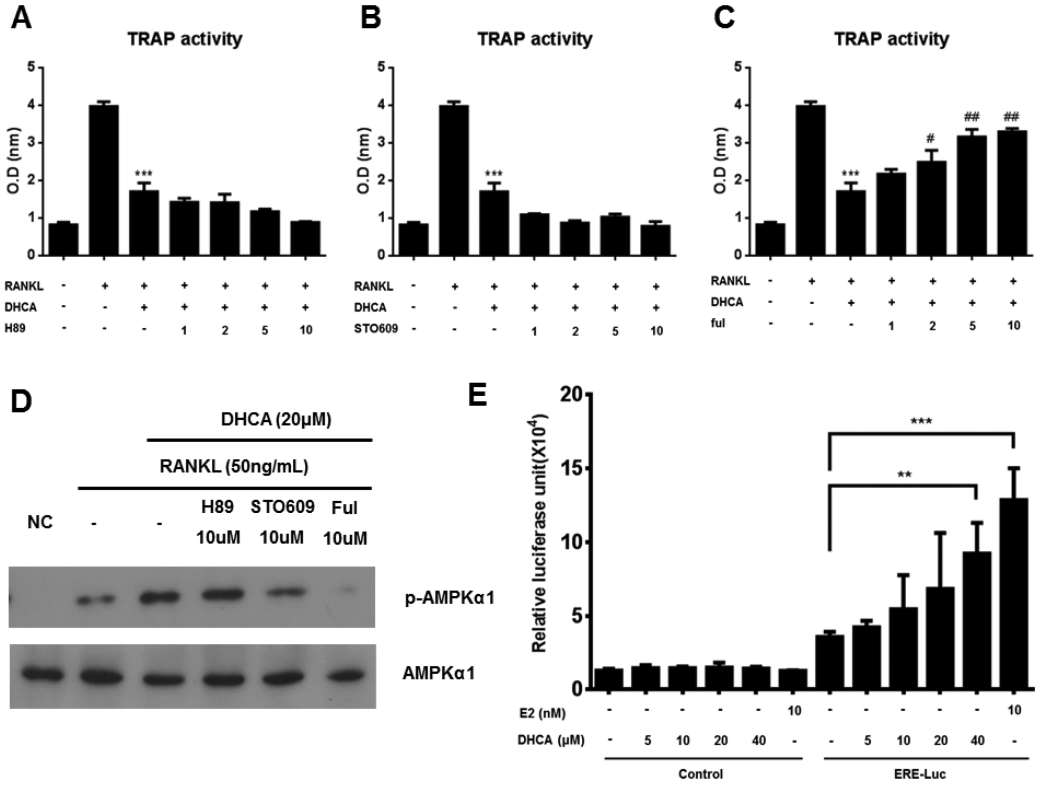

Figure 5. DHCA activates the estrogen receptor signaling pathway. (A–C) TRAP activity was measured, after 5 days, at 450 nm followed by TRAP activity assay. (D) Phosphorylation status of AMPKα1 was measured. RAW264.7 cells were cocultured with RANKL, DHCA (20 μM), and various concentrations of H89, STO609, and fulvestrant. (E) Luciferase activity was measured. RAW264.7 cells were transfected with control or luciferase reporter plasmid containing sequences for ERE, then were treated with various concentrations of DHCA or E2 (10 nM) for 6 h. Total protein was prepared, and the activity of luciferase was measured using a luminometer. Values represent the mean ± SEM of three independent experiments. $^{***}p < 0.001$ compared with that treated with RANKL alone; $^{\#}p < 0.05$, $^{\#\#}p < 0.01$ compared with that treated with RANKL and DHCA.

performed. The structures of ERα and ERβ ligand binding domains from *Mus musculus* were built using a human ER structure by homology modeling, and potential binding poses with estradiol or DHCA were generated using Glide software.[32] As shown in Figure 7A and B, DHCA was estimated to show a similar binding pose with ERα. Furthermore, the 2D ligand–receptor interaction diagram showed that intermolecular forces, such as hydrogen bonds and π–π interactions between ERα and DHCA, were analogous to the case of estradiol (Figure 7C and D). These data indicated that DHCA might bind to ERα. The same analysis predicted that DHCA might also interact with ERβ (Figure 7E–H). Consistent with these analyses, DHCA was predicted to have sufficient MM-GBSA binding energy to bind with ERα and ERβ (Table 1). Taken together, these data indicated that DHCA might have the potential to bind to the estrogen receptor family. However, the biological outcome might be different depending on cellular targets.

DHCA Acts as Agonist on Both Estrogen Receptor Alpha and Beta. To determine whether DHCA binds to the ERα and ERβ, an estrogen receptor competition assay was performed. Various concentrations of DHCA were added to estrogen receptor/fluormone tracer complex for 2 h, and the fluorescence polarization value was measured. As shown in Figure 8A and B, DHCA bound to ERα and ERβ. The IC_{50} values obtained from these experiments indicate that DHCA binds both ERα and ERβ with lower affinity than estradiol. The estimated IC_{50} values for ERα and ERβ were 61.91 and 286.5 nM, respectively (Table 2). Therefore, DHCA acts as an ERα agonist that displays 4.63-fold selectivity over ERβ; however the difference in IC_{50} between ERα and ERβ was not significant. These data indicated that DHCA might show estrogenic effects through binding to both ERα and ERβ.

DHCA Blocks Ovx-Induced Bone Loss and Decreases Osteoclastogenic Gene Expression in Bone Marrow. The above data show the potential therapeutic effects of DHCA in osteoporosis. To test this possibility, ovariectomized mice were used in which the ovary is physically removed, resulting in phenotypes similar to osteoporosis.[33] The ovary was removed on day 0, and various doses of DHCA were injected intraperitoneally on a daily basis to ovariectomized mice; femurs were analyzed by micro-CT after 4 weeks. As shown in Figure 9A and B, ovariectomized mice showed significant bone loss, and this effect was diminished upon DHCA treatment in a dose-dependent manner. The 3D-structure analysis showed that the removal of the ovaries reduced various bone morphometric parameters such as trabecular bone volume (BV/TV), trabecular thickness (Tb.Th), trabecular number (Tb.N), and bone marrow density (BMD), as compared to the control. Effects of DHCA treatment were visually clear in all these parameters (Figure 9C). Similarly, trabecular bone surface (BS/BV), trabecular spacing (Tb.Sp), trabecular pattern factor (Tb.Pf), and structure model index (SMI) were increased in the sham group, and these effects were diminished with DHCA treatment with the exception SMI (Figure 9C).

The blood level of N- or C-telopeptide of type I collagen (NTx or CTx),[34,35] a biochemical marker for bone degradation, was also measured by ELISA. DHCA decreased the blood level of NTx and CTx, which had been elevated by Ovx (Figure 9D).

DOI: 10.1021/acs.jnatprod.7b00927
J. Nat. Prod. 2018, 81, 1343–1356

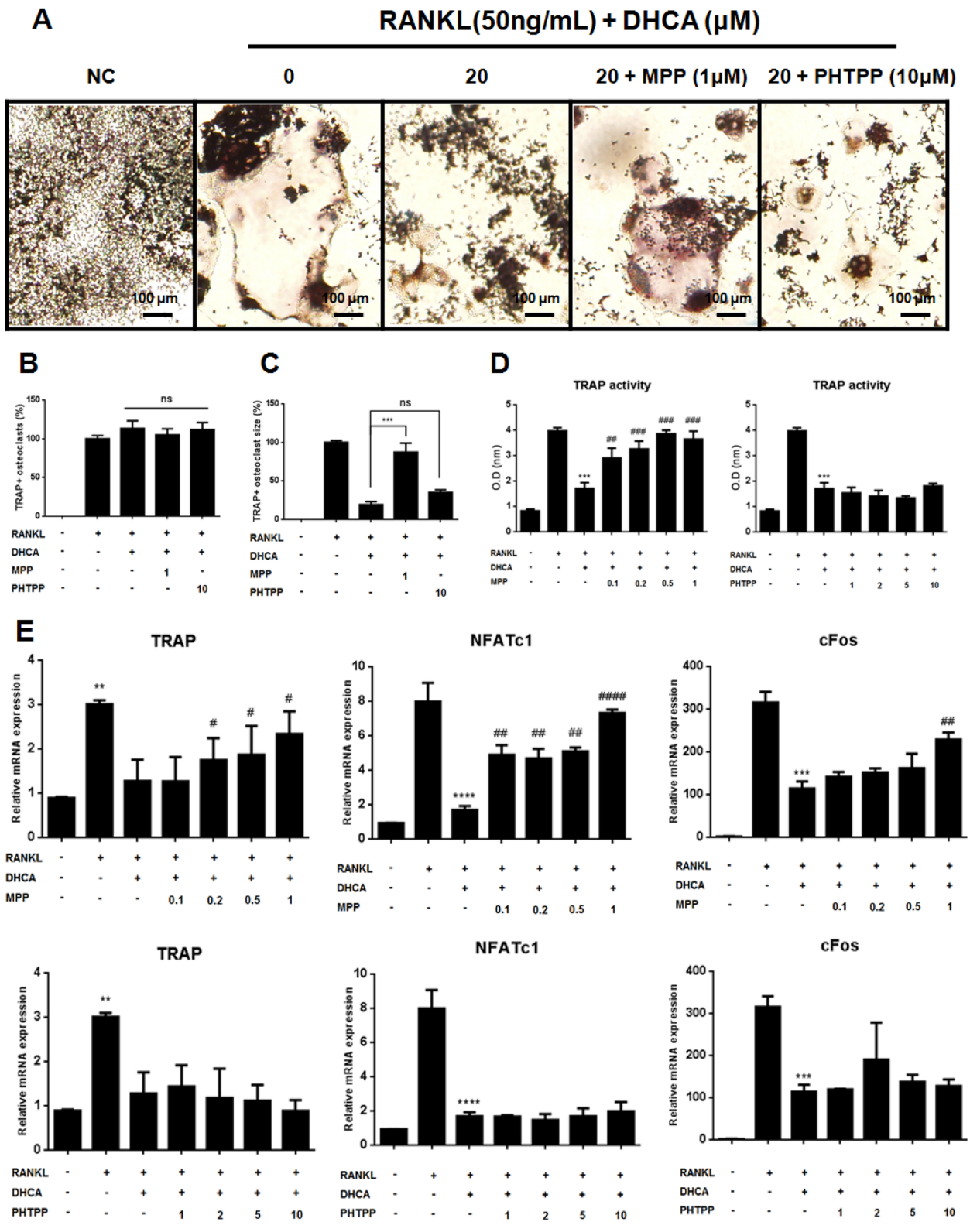

Figure 6. continued

DOI: 10.1021/acs.jnatprod.7b00927
J. Nat. Prod. 2018, 81, 1343−1356

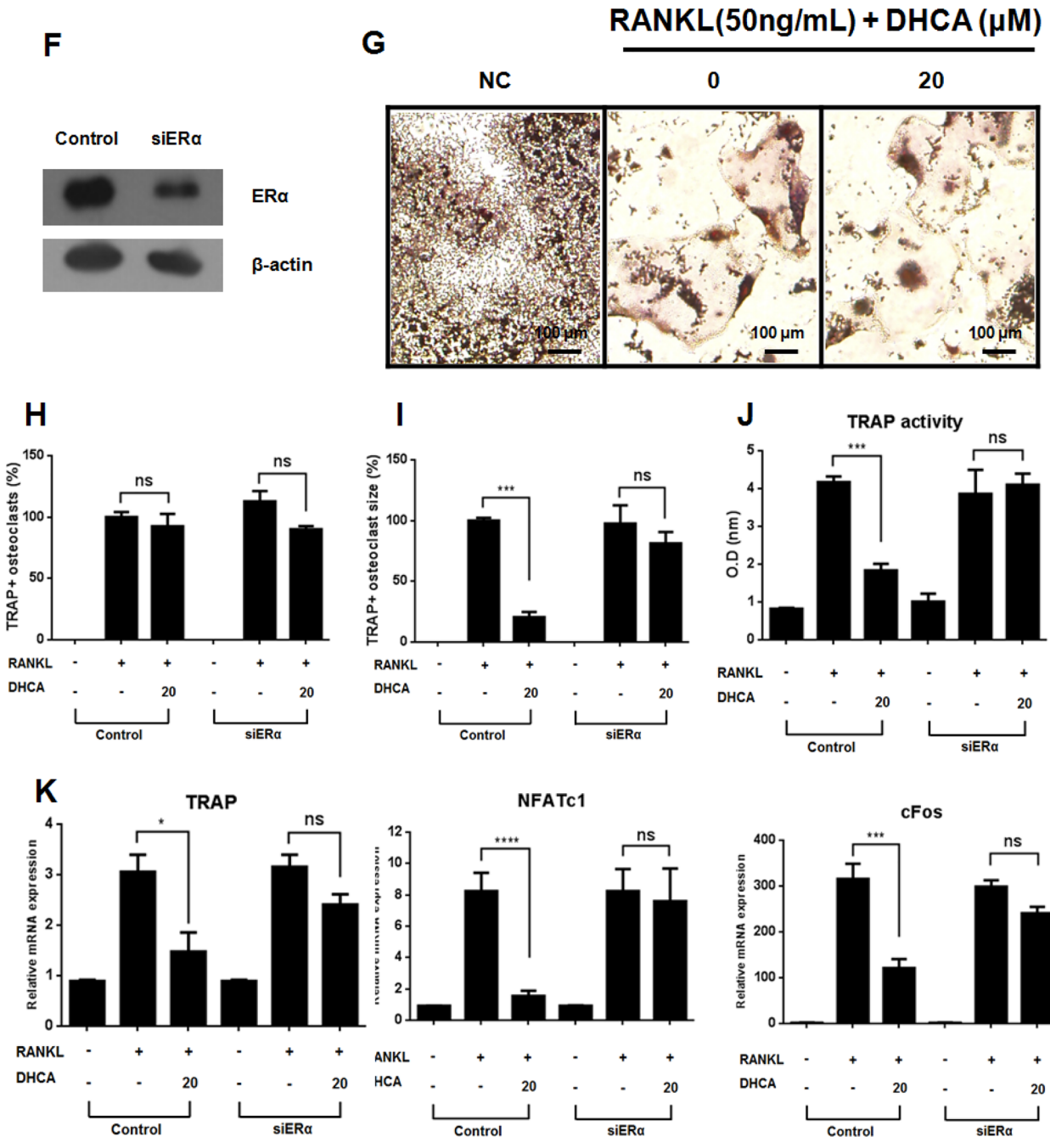

Figure 6. Anti-osteoclastogenic effects of DHCA were mediated by ERα, but not ERβ. RAW264.7 cells were cotreated with RANKL (50 ng/mL) and various concentrations of MPP (0.1−1 μM) or PHTPP (1−10 μM) and cultured in the presence of DHCA (20 μM). (A) TRAP-positive multinucleated cells were visualized by TRAP staining. (B) The number of TRAP-positive multinucleated cells was counted under the microscope. (C) The size of TRAP-positive multinucleated cells was measured under the microscope. (D) TRAP activity was measured, after 5 days, at 450 nm followed by a TRAP activity assay. (E) The expression level of osteoclastogenic genes was measured by quantitative RT-PCR after 24 h. RAW264.7 cells were transfected with ERα siRNA or control siRNA and then were cotreated with RANKL (50 ng/mL) and DHCA (20 μM). (F) The protein level of ERα was determined by Western blot. (G) TRAP-positive multinucleated cells were visualized by TRAP staining. (H) The number of TRAP-positive multinucleated cells was counted under the microscope. (I) The size of TRAP-positive multinucleated cells was measured. (J) TRAP activity was measured, after 5 days, at 450 nm followed by a TRAP activity assay. (K) The expression level of osteoclastogenic genes was measured by quantitative RT-PCR after 24 h. TRAP-stain results with control siRNA transfection are shown in Supplementary Figure 3. Values represent the mean ± SEM of three independent experiments. $^{**}p < 0.01$, $^{***}p < 0.001$, $^{****}p < 0.0001$ compared with that treated with RANKL alone; $^{\#\#}p < 0.01$, $^{\#\#\#}p < 0.001$, $^{\#\#\#\#}p < 0.0001$ compared with that treated with RANKL and DHCA.

Finally, osteoclastogenic gene expression patterns were also analyzed by measuring the RNA level of TRAP, NFATc1, cathepsin K, and c-Fos in bone marrow by quantitative RT-PCR. In the sham group, the RNA level of TRAP, NFATc1, and cathepsin K was increased, while it was significantly lowered in DHCA-treated animals (Figure 9E). Taken together, these data indicated that DHCA might inhibit bone loss mediated by estrogen deficiency.

DHCA is a lignan isolated from water-soluble extracts of *C. moschata*.[21] It was previously shown to contain potent anti-

DOI: 10.1021/acs.jnatprod.7b00927
J. Nat. Prod. 2018, 81, 1343−1356

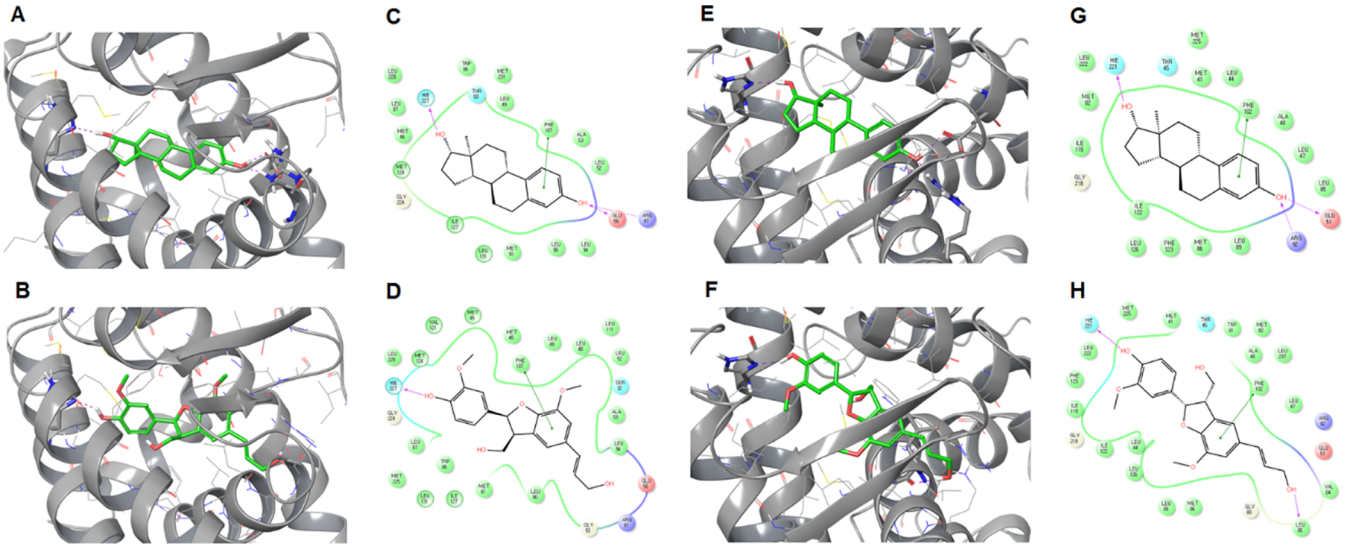

Figure 7. DHCA was predicted to bind with ERα and ERβ by molecular docking simulation. (A) Crystal structure of ERα LBD in complex with 17β-estradiol. (B) Crystal structure of ERα LBD in complex with DHCA. (C) 2D ERα−17β-estradiol interaction diagram. Hydrogen bonds (purple arrow) and $\pi-\pi$ interactions (green arrow) are shown. (D) 2D ERα−DHCA interaction diagram. (E) Crystal structure of ERβ LBD in complex with 17β-estradiol. (F) Crystal structure of ERβ LBD in complex with DHCA. (G) 2D ERβ−17β-estradiol interaction diagram. (H) 2D ERβ−DHCA interaction diagram. Ligand−receptor molecular docking was simulated by Glide (see Experimental Section).

Table 1. MM−GBSA Binding energy

receptor	ligand	MM−GBSA binding energy (kcal/mol)
ERα	DHCA	−82.449
	estradiol	−106.576
ERβ	DHCA	−83.465
	estradiol	−112.859

Table 2. IC_{50} Values

receptor	test compound	IC_{50} (nM)
ERα	estradiol	4.804
	DHCA	61.91
ERβ	estradiol	1.280
	DHCA	286.5

adipogenic,[21] anti-inflammatory,[22] and anti-oxidative activities[23] in fibroblast, macrophage, and lymphocyte cell types. DHCA is a member of the phytoestrogens, while RANKL-induced osteoclastogenesis has been shown to be inhibited by estrogen. In this study, we investigated the effects of DHCA on RANKL-induced osteoclastogenesis in RAW264.7 cells. DHCA reduced the number of TRAP-positive multinucleated cells as well as inhibited the activity of TRAP. This lignan molecule decreased the expression of various genes involved in osteoclastogenesis such as NFATc1, c-Fos, TRAP, MMP-9, DC-STAMP, and cathepsin K and suppressed the signaling pathways involving p38 MAPK and NF-κB induced by RANKL. Furthermore, DHCA increased the level of phosphorylated AMPK, while the above anti-osteoclastogenic effects of DHCA were diminished when AMPKα1 expression was knocked down using siRNA. The AMPK-activating effect of DHCA was attenuated by inhibition of ERα. The results from molecular docking simulation and receptor competition assays indicated that DHCA might act as an agonist on both ERα and ERβ. Consistent with these in vitro data, DHCA could effectively suppress bone loss and osteoclastogenesis induced by ovariectomy in the mouse model.

MAPKs are protein kinases involved in the control of cellular responses to extracellular stimuli, such as growth factors, heat shock proteins, and pro-inflammatory cytokines, and regulate a variety of biological processes including mitosis, apoptosis, and differentiation.[36] The most studied MAPKs are ERK1/2, JNKs, and p38 kinases.[37] It has recently been reported that RANKL-mediated activation of three kinases plays an important role in osteoclast differentiation.[38−40] Our data suggested that DHCA specifically suppressed the RANKL-induced p38 MAPK path-

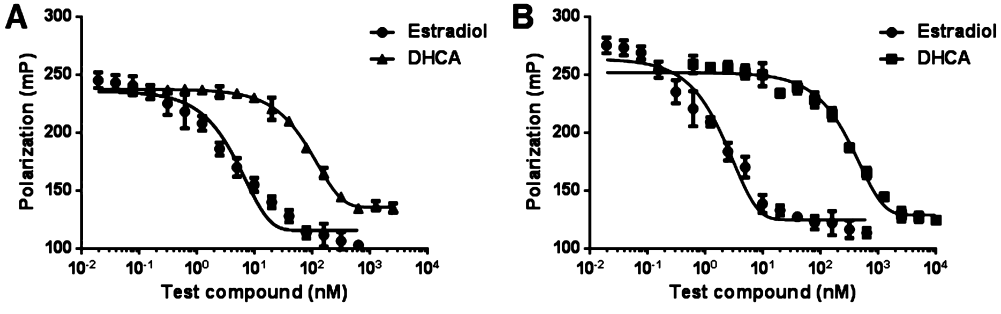

Figure 8. DHCA acts as agonist on both ERα and ERβ. (A) Polarization values for ERα against the concentration of DHCA. (B) Polarization values for ERβ against the concentration of DHCA. An estrogen receptor competition assay was performed using a PolarScreen ERα/β competitor assay kit (see Experimental Section).

DOI: 10.1021/acs.jnatprod.7b00927
J. Nat. Prod. 2018, 81, 1343−1356

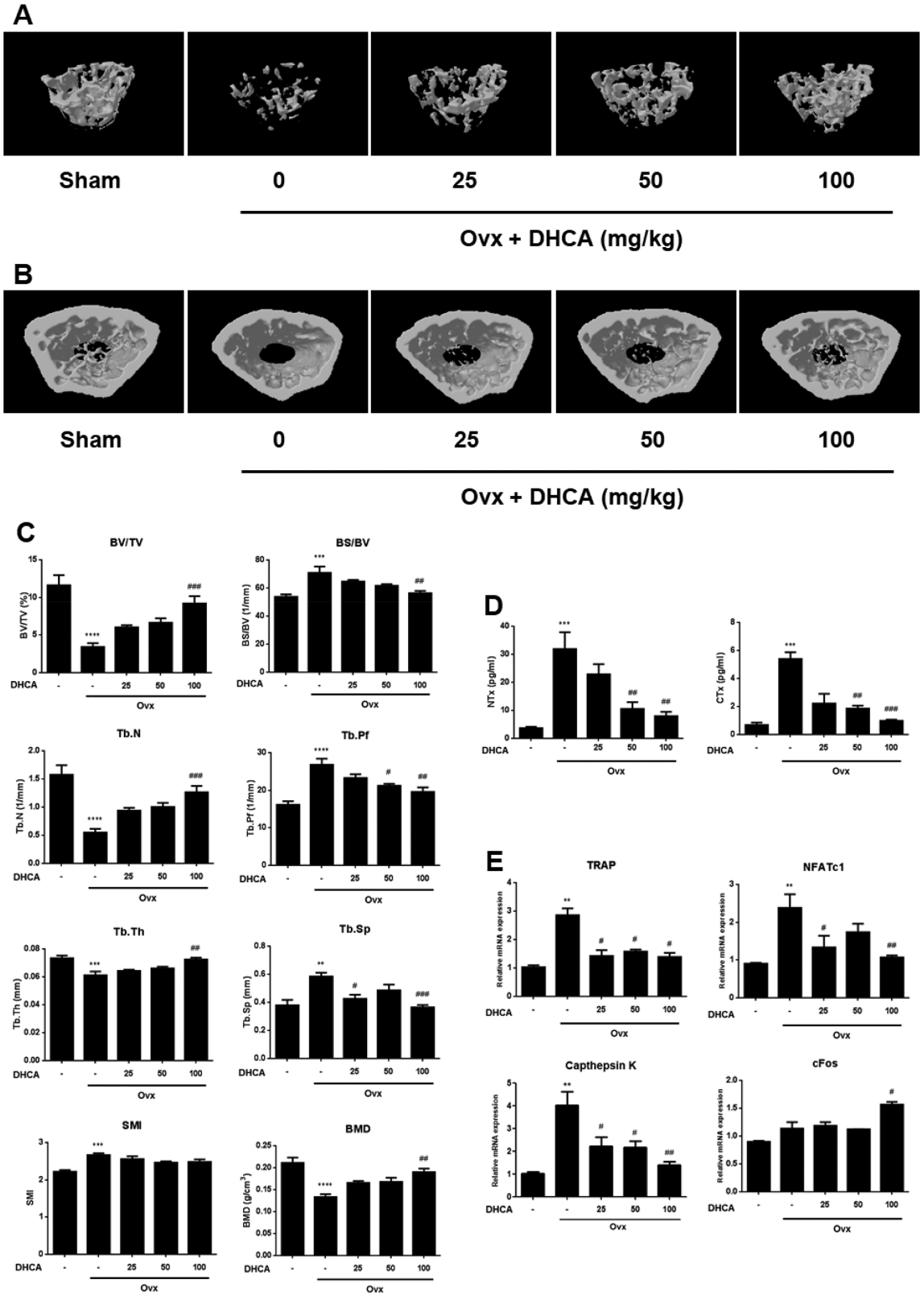

Figure 9. DHCA treatment prevents ovariectomy-induced bone loss and reduces osteoclastogenesis in bone marrow. (A) 3D structure of trabecular bone in proximal femur obtained by μCT. (B) 2D image of proximal femur obtained by μCT. (C) Bone volume over total volume (BV/TV, %), bone surface density (BS/BV, 1/mm), trabecular thickness (Tb.Th, mm), trabecular spacing (Tb.Sp, mm), trabecular number (TB.N, 1/mm), trabecular pattern factor (TB.Pf, 1/mm), structure model index (SMI), and bone mineral density (BMD, g/cm^3) obtained by μCT. (D) Serum NTx and CTx measured by ELISA. (E) Osteoclastogenic gene expression in bone marrow measured by quantitative RT-PCR; 7-week-old Balb/c mice were subjected to sham operation or OVX, then vehicle or various doses of DHCA were injected i.p. for 4 weeks. Values represent the mean ± SEM of three independent experiments. $^{**}p < 0.01$, $^{***}p < 0.001$ compared with control group; $^{\#}p < 0.05$, $^{\#\#}p < 0.01$, $^{\#\#\#}p < 0.001$ compared with Ovx group.

DOI: 10.1021/acs.jnatprod.7b00927
J. Nat. Prod. 2018, 81, 1343−1356

way, but not pathways involving ERK1/2 and JNK, indicating that DHCA might interact with upstream proteins of the p38 pathway. Examples include MAPKK kinases (MAPKKKs), such as MEKKs 1 to 4, MLK2 and -3, and Tak1, or MAPK kinases (MAPKKs) such as MEK3 and MEK6.[41,42] It is also possible that DHCA directly interacts with p38 as in the case of SB203580, a pyridinyl imidazole compound that binds to the ATP binding pocket of p38, thereby regulating its phosphorylation status.[43]

The fact that DHCA activates AMPK is important for several reasons. First, activation of AMPK has been shown to activate Runx2, a master regulator in the process of osteoblastogenesis.[44] Since DHCA can also down-regulate the expression of various genes involved in osteoclastogenesis, DHCA may be a very effective agent that can suppress bone loss by controlling both bone resorption and bone formation. Second, DHCA may be a more specific regulator as compared with other plant-derived compounds known to activate AMPK such as resveratrol, curcumin, and catechin.[45−47] These proteins have been reported to activate all three MAPK pathways including ERK1/2, JNKs, and p38 kinases.[48,49] However, DHCA affected only p38 kinases, but not ERK1/2 or JNK, and thus might have fewer side effects than other plant-derived compounds.

It has been previously reported that estradiol has anti-osteoclastogenic activity via activation of AMPK.[19] On the basis of this result, we performed experiments to determine whether anti-osteoclastogenic effects of DHCA are mediated through binding to the estrogen receptor. Data from experiments involving siRNAs specific for ERα and ERβ indicated that the effects of DHCA were mediated by ERα, not ERβ. Interestingly, molecular docking simulation performed between DHCA and estrogen receptors predicted that DHCA might bind efficiently to ERα and ERβ. Consistent with this prediction, an estrogen receptor competition assay revealed that DHCA might act as a potent agonist for both ERα and ERβ, probably with a relatively small difference in binding affinity. One possible explanation is the difference in tissue distribution of these two estrogen receptors.[50] ERα is known to be expressed at preosteoclast stages, whereas ERβ is expressed at all stages.[51] Therefore, the anti-osteoclastogenic effects of DHCA might have been mediated mainly by ERα. If this is indeed the case, DHCA may produce different effects in other tissues or cell types.

Our data from TRAP-staining analysis showed that DHCA affected the size of osteoclasts rather than their number. This may have important implications, as cell−cell fusion in osteoclasts is considered to play a critical role in osteoclast functions through reorganization of the cytoskeleton.[52] Among three key players (DC-STAMP,[53] OC-STAMP,[54] and P2X7 receptors[55]) known to be involved in cell−cell fusion during osteoclastogenesis, DC-STAMP, at least, seems to be a candidate cellular target of DHCA, because the RNA level of DC-STAMP was reduced in a concentration-dependent manner when RAW264.7 cells were treated with DHCA. It remains to be elucidated whether DHCA can also influence the expressions of two other genes.

Thus far, hormone replacement therapy involving synthetic 17β-estradiol or conjugated equine estrogens has been commonly used to treat postmenopausal osteoporosis.[56] However, there have been safety concerns since the use of such synthetic estrogens might increase the risk of hormone-dependent cancers and cardiovascular diseases.[57] In this regard, phytoestrogens have been explored as a possible alternative to synthetic estrogens.[57] Many well-known phytoestrogens show a higher affinity for ERβ, whereas synthetic estrogens more preferentially bind to ERα.[58] It has been argued that phytoestrogens may be safer than synthetic estrogens, as ERβ signaling inhibits mammalian cell growth.[59] Furthermore, it has been suggested that phytoestrogens may provide other safety benefits thanks to their antioxidant activities independent of ER.[60] DHCA seems to bind to both ERα and ERβ with a similar degree of affinity while generating potent antioxidant activities via up-regulation of HO-1.[23] It remains to be seen whether such characteristics of DHCA could act as a positive or negative factor in developing this lignan molecule as a therapeutic agent for osteoporosis. Given the effective suppression of bone loss and osteoclastogenesis by DHCA, far more extensive *in vitro* and *in vivo* characterizations of the phytoestrogen molecule are warranted.

EXPERIMENTAL SECTION

Cell Culture and Reagents. Synthetic DHCA was produced by previously described methods[61] and obtained from Biochemnet (Seoul, Korea). RAW264.7 cells were purchased from the American Type Culture Collection (Manassas, VA, USA). Cells were cultured in Minimum Essential Medium Alpha (Gibco, Grand Island, NY, USA) containing 10% fetal bovine serum (FBS, Hyclone, Logan, UT, USA) and antibiotics (100 U/mL penicillin and 100 mg/mL streptomycin) at 37 °C under 5% CO_2. RANKL, L-ascorbic acid, sodium tartrate dehydrate, 4-nitrophenyl phosphate sodium, 17β-estradiol, H89, STO609, and fulvestrant were purchased from Sigma (St Louis, MO, USA), while MPP and PHTPP were from R&D Systems (Minneapolis, MN, USA).

Experimental Animals. All animal protocols were performed in compliance with the guidelines set by the Institutional Animal Care and Use Committee of Seoul National University. Female 8-week-old Balb/c mice were purchased from Orientbio Inc. (Seongnam, Korea) and housed in an air-conditioned facility at Seoul National University with a fixed 12 h light/dark cycle.

All animal experiments were carried out in accordance with the Guide for Animal Experimentation of Seoul National University. The protocol was approved by the Institutional Animal Care and Use Committee of Seoul National University.

Osteoclast Differentiation *in Vitro*. For osteoclast differentiation experiments, RAW264.7 cells were plated at 3×10^3 cells per well in 96-well culture plates containing α-MEM with 10% FBS. Twenty-four hours later, cells were treated with 50 ng/mL of RANKL and various concentrations of DHCA. After 5 days in culture, the cells were subjected to an acid phosphatase leukocyte (TRAP) kit (Sigma) according to the manufacturer's instructions.

Measuring TRAP Activity. After osteoclast differentiation, TRAP activities of osteoclasts were measured in the well by incubating them for 15−30 min at 37 °C with 30 μL of 600 mM sodium acetate buffer (pH 5.5) containing L-ascorbic acid (17.6 mg/mL), sodium tartrate dehydrate (9.2 mg/mL), 4-nitrophenylphosphate Na (3.6 mg/mL), Triton X-100 (0.3%), EDTA (6 mM), and NaCl (600 mM). The reaction was terminated by the addition of 30 μL of NaOH (300 mM), and activities were measured at 405 nm.

MTT Assay. The MTT assay was performed as described previously.[22] Briefly, RAW264.7 cells were treated with RANKL (50 ng/mL) or various concentrations of DHCA for 24 to 72 h. Cells were then incubated with an MTT labeling reagent for 4 h followed by the addition of solubilization solution. After 24 h, cytotoxicity was determined by measuring the OD at 550 nm using an ELISA microplate reader.

Pit Formation Assay. Pit formation assay was performed using an osteoassay plate (Corning, NY, USA). RAW264.7 cells were seeded on an osteoassay plate and cocultured with RANKL and various concentrations of DHCA for 7 days. The culture medium was then aspirated completely followed by incubation in a 10% bleach solution for 5 min. Pit formation was observed under an optic microscope (Olympus, Tokyo, Japan).

DOI: 10.1021/acs.jnatprod.7b00927
J. Nat. Prod. 2018, 81, 1343−1356

Quantitative Reverse Transcription Polymerase Chain Reaction (qRT-PCR) Analysis. After 24 h in osteoclast differentiation, total RNA was isolated using TRIzol reagent (Invitrogen, Carlsbad, CA, USA) according to the manufacturer's protocol. cDNA was synthesized using an oligodT primer (Qiagen, Valencia, CA, USA) and AMV reverse transcriptase (TaKaRa, Shiga, Japan). One microliter of this cDNA per sample was used for quantitative polymerase chain reaction using SYBR Premix Ex TaqTM (TaKaRa, Shiga, Japan). The primer sequences used in this study were [forward, GGT CAG CAG CTC CCT AGA AG; reverse, GGA GTG GGA GCC ATA TGA TTT] for TRAP, [forward, ACT TCT TGT TTC CGG C; reverse, AGC TTC AGG GTA GGT G] for c-Fos, [forward, GGA GAG TCC GAG AAT CGA GAT; reverse, TTG CAG CTA GGA AGT ACG TCT] for NFATc1, [forward, GGA CCC GAA GCG GAC ATT G; reverse, GAA GGG ATA CCC GTC TCC GT] for MMP-9, [forward, CCA AGG AGT CGT CCA TGA TT; reverse, GGC TGC TTT GAT CGT TTC TC] for DC-STAMP, and [forward, AGG CAG CTA AAT GCA GAG GGT ACA; reverse, ATG CCG CAG GCG TTG TTC TTA TTC] for cathepsin K. Conditions for PCR were denaturation at 95 °C for 5 s and annealing and extension at 60 °C for 20 s.

Western Blot Analysis. RAW264.7 cells were plated in 100 mm culture dishes. Twenty-four hours later, cells were treated with RANKL (50 ng/mL) and various concentrations of DHCA for 30 min. After treatment, cells were washed with cold phosphate-buffered saline (PBS) and lysed with phosphosafe extraction buffer (Novagen, Madison, WI, USA). Total proteins were separated by SDS-PAGE and electrophoretically transferred to PVDF membranes. The membranes were incubated with primary antibodies against p-Akt (1:500, Cell Signaling, Beverly, MA, USA), Akt (1:1000, Cell Signaling), p-IKKβ (1:500, Santa Cruz Biotechnology, Santa Cruz, CA, USA), IKKβ (1:500, Santa Cruz), IκB (1:500, Santa Cruz), p-JNK (1:1000, Cell Signaling), JNK (1:1000, Cell Signaling), p-p38 (1:1000, Cell Signaling), p38 (1:1000, Cell Signaling), p-ERK (1:1000, Cell Signaling), ERK (1:1000, Cell Signaling), p-AMPKα1 (1:1000, Cell Signaling), AMPKα1 (1:1000, Cell Signaling), and β-actin (1:5000, Sigma). Membranes were then treated with horseradish peroxidase-conjugated anti-mouse or anti-rabbit IgG (1:100 000, Sigma) and visualized in films using ECL solution (Millipore, Billerica, MA, USA).

Preparation of Nuclear Proteins. RAW264.7 cells were plated in 100 mm culture dishes. Twenty-four hours later, cells were treated with RANKL (50 ng/mL) and various concentrations of DHCA for 24 h. After treatment, cells were washed with cold PBS and lysed with 200 μL of lysis buffer A [10 mM HEPES (pH 7.9), 10 mM KCl, 1.5 mM $MgCl_2$, 0.1 mM EDTA, and 1 mM dithiothreitol] and incubated on ice for 20 min. Twenty microliters of lysis buffer B (lysis buffer A containing 0.5% Nonidet-P40) was added for another 20 min to disrupt cell membranes, followed by centrifugation at 5000g for 5 min. Crude nuclei were resuspended in 20 μL of lysis buffer C [10 mM HEPES (pH 7.9), 400 mM NaCl, 1.5 mM $MgCl_2$, 1 mM EDTA, 1 mM dithiothreitol] and incubated on ice for 1 h. The nuclear proteins were obtained by centrifugation at 16000g for 10 min.

siRNA Transfection. The siRNA specific for AMPKα1, ERα, ERβ, and scrambled siRNA were purchased from Santa Cruz Biotechnology. The siRNA was transfected into RAW264.7 cells using the RNAiMAX (ThermoFisher Scientific, Woburn, MA, USA) according to the manufacturer's protocol. After 48 h, the cells were subjected to the analysis. Knock-down efficiency was evaluated using primary antibodies against AMPKα1 (1:1000, Cell Signaling), ERα (1:1000, Cell Signaling), and ERβ (1:1000, Cell Signaling).

Luciferase Reporter Plasmid Assay. Inducible ERE-responsive luciferase reporter plasmid was purchased from Qiagen. The luciferase reporter plasmid assay was performed as described previously.[22] Briefly, RAW264.7 cells were transiently transfected with ERE-reporter plasmid and a β-galactosidase plasmid (1 μg, Invitrogen), using Lipofectamine 2000 (Invitrogen) according to the manufacturer's protocol. Twenty-four hours after transfection, the cells were treated with 17β-estradiol (10 nM) and various concentrations of DHCA for 24 h. Cell lysates were prepared, and a luciferase activity assay was performed using the luciferase reporter kit according to the manufacturer's protocol (Promega, Madison, WI, USA) with a microplate luminometer (MicroLumatPlus LB96 V, Berthold, Germany). Luciferase activity was normalized to β-gal activity.

Sequence Alignment and Homology Modeling. The amino acid sequences of ERα and ERβ for *Mus musculus* (mERα and mERβ, accession number: BAJ65337 and AAB51132) and *Homo sapiens* (hERα and hERβ, accession number: 2OCF_A and 2J7X_A) were retrieved from the NCBI protein sequence database. Global pairwise sequence alignment of mERα and mERβ amino acid sequences was performed using the EMBOSS package to calculate sequence identity and similarity among the species. To identify a suitable template, the amino acid sequences of mERα and mERβ were searched against the Protein Data Bank (PDB) database using the PSI-BLAST algorithm. The crystal structures of hERα for mERα and hERβ for mERβ (PDB ID: 2OCF and 2J7X) were used as templates to build mERα and mERβ structures. Homology modeling of the mERα and mERβ was performed using the Prime homology modeling program of Schrödinger. The crystallographic positions of the backbone atoms and conserved side chains were mapped from the template, while the side chain coordinates of all nonidentical residues were predicted.

Molecular Docking Simulation. Ligand−receptor molecular docking was simulated by Glide (Schrödinger). The grid-generation module from Glide was used to generate grids for the mERα and mERβ structures produced through homology modeling. The scaling factor of the van der Waals radii was set to 0.8, and the partial charge cutoff to 0.15. The binding site of mERα or mERβ was included in the grid generation. Dehydrodiconiferyl alcohol and estradiol, the selected ligands, were drawn by 2D Sketcher and optimized with MacroModel. All possible ionization states and stereoisomer structures of the ligands were generated using the Ionizer option in LigPrep. Five poses per ligand, while performing the docking of these two compounds to mERα and mERβ, were produced by the SP mode of Glide, respectively. The ligand interaction diagram module of Glide was used to analyze ligand−protein interactions.

Calculation of Binding Energy. The Prime molecular mechanics based generalized Born/surface area (MM-GBSA) model of the Schrödinger suite was used to calculate the free energy of binding of the ER−ligand complex from the docking simulations. The binding free energy (ΔG_{bind}) was evaluated as

$$\Delta G_{bind} = \Delta E_{MM} + \Delta G_{solv} + \Delta G_{SA}$$

where ΔE_{MM} is the difference in the minimized energies between the ER−ligand complex and the sum of the energies of the free ER and ligand. ΔG_{solv} is the difference between the GBSA solvation energy of the ER−ligand complex and the sum of the solvation energies of free ER and ligand. ΔG_{SA} is the difference between the surface area energies of the complex and the sum of the surface area energies of free ER and ligand.

Estrogen Receptor Competition Assay. The estrogen receptor competition assay was performed using the PolarScreen ERα/β competitor assay kit (ThermoFisher Scientific) according to the manufacturer's protocol. Briefly, a 2× solution of estrogen receptor/Fluormone tracer complex in a 384-well polypropylene black microplate (Corning, NY, USA) was prepated, and a test compound was added immediately using a multichannel pipet, then incubated for 2 h. Fluorescence polarization values were measured using a FlexStation 3 multi-mode microplate reader (Molecular Devices, Sunnyvale, CA, USA).

Ovariectomized-Mice Model. Ovariectomy surgery was performed as described previously.[62] Briefly, all mice were housed and given 1 week to adapt to their surroundings before surgery. The experimental groups were divided into five groups (sham surgery with vehicle, ovariectomy with vehicle, and ovariectomy with various concentrations of DHCA; n = 10 mice per group). Sham mice underwent bilateral laparotomy, but the ovaries were left in place, while mice in the other four groups underwent bilateral ovariectomy via the ventral approach. After a week of recuperation, all treatments were given by intraperitoneal route and continued for 4 weeks. At the completion of the study, animals were necropsied, and serum samples and femur bones were collected. Serum samples were subjected to NTx (Cusabio, Wuhan, China) and CTx (Cusabio) ELISA according to the

DOI: 10.1021/acs.jnatprod.7b00927
J. Nat. Prod. 2018, 81, 1343−1356

manufacturer's protocol. Bone marrow was flushed out from femur bones, total RNA from bone marrow was isolated using TRIzol reagent (Invitrogen), and quantitative RT-PCR was performed. Bones were kept in formalin solution for μCT study. 3D and 2D trabecular structure and parameters such as bone volume over total volume (BV/TV, %), bone surface density (BS/BV, 1/mm), trabecular thickness (Tb.Th, mm), trabecular spacing (Tb.Sp, mm), trabecular number (TB.N, 1/mm), trabecular pattern factor (Tb.Pf, 1/mm), structure model index (SMI), and bone mineral density (BMD, g/cm^3) were calculated.

Statistical Analysis. All quantitative data were presented as means ± SEM from three independent experiments. Differences between two groups were statistically analyzed using Student's *t* test, whereas one-way ANOVA was used for multiple comparisons. *P*-values were calculated and when less than 0.05 were considered to be statistically significant.

■ ASSOCIATED CONTENT

Supporting Information

The Supporting Information is available free of charge on the ACS Publications website at DOI: 10.1021/acs.jnatprod.7b00927.

Additional information (PDF)

■ AUTHOR INFORMATION

Corresponding Author

*Tel: +82-2-880-8015. E-mail: sunyoung@snu.ac.kr.

ORCID

Wonwoo Lee: 0000-0003-4186-8888

Sunyoung Kim: 0000-0002-1736-9088

Notes

The authors declare no competing financial interest.

■ ACKNOWLEDGMENTS

The authors thank Quantum Bio Solutions (Seoul, Korea) for performing the homology remodeling, molecular docking simulation, and calculation of binding energy. This work was supported by three research grants: (1) 2012008018 (National Research Foundation of Korea), (2) 2012K001130 (Brain Research Center of 21st Century Frontier Research Program), and (3) the industry/academy cooperation research grant from ViroMed Co. Ltd. The first two are administered by the Ministry of Education, Science and Technology, Korea.

■ REFERENCES

(1) Kanis, J. A. *Lancet* **2002**, *359*, 1929−1936.
(2) Gardner, M. J.; Demetrakopoulos, D.; Shindle, M. K.; Griffith, M. H.; Lane, J. M. *HSS J.* **2006**, *2*, 62−69.
(3) Wright, N. C.; Looker, A. C.; Saag, K. G.; Curtis, J. R.; Delzell, E. S.; Randall, S.; Dawson-Hughes, B. *J. Bone Miner. Res.* **2014**, *29*, 2520−2526.
(4) Wilkins, C. H. *Clin. Interventions Aging* **2007**, *2*, 389−394.
(5) Vondracek, S. F.; Linnebur, S. A. *Clin. Interventions Aging* **2009**, *4*, 121−136.
(6) Iqbal, J.; Sun, L.; Zaidi. *Curr. Osteoporos Rep* **2010**, *8*, 163−167.
(7) Bauss, F.; Schimmer, R. C. *Ther. Clin. Risk Manag.* **2006**, *2*, 3−18.
(8) Messalli, E. M.; Scaffa, C. *Int. J. Women's Health* **2010**, *1*, 11−20.
(9) Riggs, B. L. *J. Clin. Invest.* **2000**, *106*, 1203−1204.
(10) Everts, V.; Korper, W.; Hoeben, K. A.; Jansen, I. D.; Bromme, D.; Cleutjens, K. B.; Heeneman, S.; Peters, C.; Reinheckel, T.; Saftig, P.; Beertsen, W. *J. Bone Miner. Res.* **2006**, *21*, 1399−1408.
(11) Soysa, N. S.; Alles, N. *Biochem. Biophys. Res. Commun.* **2009**, *378*, 1−5.
(12) Lee, K.; Chung, Y. H.; Ahn, H.; Kim, H.; Rho, J.; Jeong, D. *Int. J. Biol. Sci.* **2016**, *12*, 235−245.
(13) Kim, J. H.; Kim, N. *J. Bone Metab* **2014**, *21*, 233−241.
(14) Choi, S. W.; Park, K. I.; Yeon, J. T.; Ryu, B. J.; Kim, K. J.; Kim, S. H. *BMC Complementary Altern. Med.* **2014**, *14*, 35.
(15) Takayanagi, H.; Kim, S.; Koga, T.; Nishina, H.; Isshiki, M.; Yoshida, H.; Saiura, A.; Isobe, M.; Yokochi, T.; Inoue, J.; Wagner, E. F.; Mak, T. W.; Kodama, T.; Taniguchi, T. *Dev. Cell* **2002**, *3*, 889−901.
(16) Shah, M.; Kola, B.; Bataveljic, A.; Arnett, T. R.; Viollet, B.; Saxon, L.; Korbonits, M.; Chenu, C. *Bone* **2010**, *47*, 309−319.
(17) Shevde, N. K.; Bendixen, A. C.; Dienger, K. M.; Pike, J. W. *Proc. Natl. Acad. Sci. U. S. A.* **2000**, *97*, 7829−7834.
(18) Clowes, J. A.; Riggs, B. L.; Khosla, S. *Immunol. Rev.* **2005**, *208*, 207−227.
(19) Nakamura, T.; Imai, Y.; Matsumoto, T.; Sato, S.; Takeuchi, K.; Igarashi, K.; Harada, Y.; Azuma, Y.; Krust, A.; Yamamoto, Y.; Nishina, H.; Takeda, S.; Takayanagi, H.; Metzger, D.; Kanno, J.; Takaoka, K.; Martin, T. J.; Chambon, P.; Kato, S. *Cell* **2007**, *130*, 811−823.
(20) Al-Anazi, A. F.; Qureshi, V. F.; Javaid, K.; Qureshi, S. *J. Nat. Sci. Biol. Med.* **2011**, *2*, 154−163.
(21) Lee, J.; Kim, D.; Choi, J.; Choi, H.; Ryu, J. H.; Jeong, J.; Park, E. J.; Kim, S. H.; Kim, S. *J. Biol. Chem.* **2012**, *287*, 8839−8851.
(22) Lee, J.; Choi, J.; Kim, S. *Br. J. Pharmacol.* **2015**, *172*, 3353−3369.
(23) Lee, J.; Kim, S. *Toxicol. Appl. Pharmacol.* **2014**, *281*, 87−100.
(24) Ballanti, P.; Minisola, S.; Pacitti, M. T.; Scarnecchia, L.; Rosso, R.; Mazzuoli, G. F.; Bonucci, E. *Osteoporosis Int.* **1997**, *7*, 39−43.
(25) Ohshiba, T.; Miyaura, C.; Inada, M.; Ito, A. *Br. J. Cancer* **2003**, *88*, 1318−1326.
(26) Liou, S. F.; Hsu, J. H.; Lin, I. L.; Ho, M. L.; Hsu, P. C.; Chen, L. W.; Chen, I. J.; Yeh, J. L. *PLoS One* **2013**, *8*, e69468.
(27) Huang, H.; Chang, E. J.; Ryu, J.; Lee, Z. H.; Lee, Y.; Kim, H. H. *Biochem. Biophys. Res. Commun.* **2006**, *351*, 99−105.
(28) Boyce, B. F.; Yamashita, T.; Yao, Z.; Zhang, Q.; Li, F.; Xing, L. *J. Bone Miner. Metab.* **2005**, *23* (Suppl), 11−15.
(29) Lee, Y. S.; Kim, Y. S.; Lee, S. Y.; Kim, G. H.; Kim, B. J.; Lee, S. H.; Lee, K. U.; Kim, G. S.; Kim, S. W.; Koh, J. M. *Bone* **2010**, *47*, 926−937.
(30) Oseni, T.; Patel, R.; Pyle, J.; Jordan, V. C. *Planta Med.* **2008**, *74*, 1656−1665.
(31) Bord, S.; Horner, A.; Beavan, S.; Compston, J. *J. Clin. Endocrinol. Metab.* **2001**, *86*, 2309−2314.
(32) Shen, J.; Zhang, W.; Fang, H.; Perkins, R.; Tong, W.; Hong, H. *BMC Bioinf.* **2013**, *14*, S6.
(33) Jee, W. S.; Yao, W. *J. Musculoskelet Neuronal Interact.* **2001**, *1*, 193−207.
(34) Hankenson, K. D.; James, I. E.; Apone, S.; Stroup, G. B.; Blake, S. M.; Liang, X.; Lark, M. W.; Bornstein, P. *Matrix Biol.* **2005**, *24*, 362−370.
(35) Katsumata, S.; Wolber, F. M.; Tadaishi, M.; Tousen, Y.; Ishimi, Y.; Kruger, M. C. *J. Nutr. Sci. Vitaminol.* **2015**, *61*, 332−337.
(36) Pearson, G.; Robinson, F.; Beers Gibson, T.; Xu, B. E.; Karandikar, M.; Berman, K.; Cobb, M. H. *Endocr. Rev.* **2001**, *22*, 153−183.
(37) Coulombe, P.; Meloche, S. *Biochim. Biophys. Acta, Mol. Cell Res.* **2007**, *1773*, 1376−1387.
(38) Lee, M. S.; Kim, H. S.; Yeon, J. T.; Choi, S. W.; Chun, C. H.; Kwak, H. B.; Oh, J. *J. Immunol.* **2009**, *183*, 3390−3399.
(39) David, J. P.; Sabapathy, K.; Hoffmann, O.; Idarraga, M. H.; Wagner, E. F. *J. Cell Sci.* **2002**, *115*, 4317−4325.
(40) Li, X.; Udagawa, N.; Itoh, K.; Suda, K.; Murase, Y.; Nishihara, T.; Suda, T.; Takahashi, N. *Endocrinology* **2002**, *143*, 3105−3113.
(41) Hommes, D. W.; Peppelenbosch, M. P.; van Deventer, S. J. *Gut* **2003**, *52*, 144−151.
(42) Roux, P. P.; Blenis, J. *Microbiol Mol. Biol. Rev.* **2004**, *68*, 320−344.
(43) Young, P. R.; McLaughlin, M. M.; Kumar, S.; Kassis, S.; Doyle, M. L.; McNulty, D.; Gallagher, T. F.; Fisher, S.; McDonnell, P. C.; Carr, S. A.; Huddleston, M. J.; Seibel, G.; Porter, T. G.; Livi, G. P.; Adams, J. L.; Lee, J. C. *J. Biol. Chem.* **1997**, *272*, 12116−12121.
(44) Jang, W. G.; Kim, E. J.; Lee, K. N.; Son, H. J.; Koh, J. T. *Biochem. Biophys. Res. Commun.* **2011**, *404*, 1004−1009.
(45) He, X.; Andersson, G.; Lindgren, U.; Li, Y. *Biochem. Biophys. Res. Commun.* **2010**, *401*, 356−362.

DOI: 10.1021/acs.jnatprod.7b00927
J. Nat. Prod. 2018, 81, 1343−1356

(46) Kim, W. K.; Ke, K.; Sul, O. J.; Kim, H. J.; Kim, S. H.; Lee, M. H.; Kim, H. J.; Kim, S. Y.; Chung, H. T.; Choi, H. S. *J. Cell. Biochem.* **2011**, *112*, 3159−3166.
(47) Oka, Y.; Iwai, S.; Amano, H.; Irie, Y.; Yatomi, K.; Ryu, K.; Yamada, S.; Inagaki, K.; Oguchi, K. *J. Pharmacol. Sci.* **2012**, *118*, 55−64.
(48) Klinge, C. M.; Blankenship, K. A.; Risinger, K. E.; Bhatnagar, S.; Noisin, E. L.; Sumanasekera, W. K.; Zhao, L.; Brey, D. M.; Keynton, R. S. *J. Biol. Chem.* **2005**, *280*, 7460−7468.
(49) Syed Hussein, S. S.; Kamarudin, M. N.; Kadir, H. A. *Am. J. Chin. Med.* **2015**, *43*, 927−952.
(50) Bottner, M.; Thelen, P.; Jarry, H. *J. Steroid Biochem. Mol. Biol.* **2014**, *139*, 245−251.
(51) Krum, S. A.; Miranda-Carboni, G. A.; Hauschka, P. V.; Carroll, J. S.; Lane, T. F.; Freedman, L. P.; Brown, M. *EMBO J.* **2008**, *27*, 535−545.
(52) Miyamoto, T. *Keio J. Med.* **2011**, *60*, 101−105.
(53) Yagi, M.; Miyamoto, T.; Sawatani, Y.; Iwamoto, K.; Hosogane, N.; Fujita, N.; Morita, K.; Ninomiya, K.; Suzuki, T.; Miyamoto, K.; Oike, Y.; Takeya, M.; Toyama, Y.; Suda, T. *J. Exp. Med.* **2005**, *202*, 345−351.
(54) Yang, M.; Birnbaum, M. J.; MacKay, C. A.; Mason-Savas, A.; Thompson, B.; Odgren, P. R. *J. Cell. Physiol.* **2008**, *215*, 497−505.
(55) Pellegatti, P.; Falzoni, S.; Donvito, G.; Lemaire, I.; Di Virgilio, F. *FASEB J.* **2011**, *25*, 1264−1274.
(56) Shintani, M. *Clin. Calcium* **2002**, *12*, 1306−1311.
(57) Moreira, A. C.; Silva, A. M.; Santos, M. S.; Sardao, V. A. *J. Steroid Biochem. Mol. Biol.* **2014**, *143*, 61−71.
(58) Sunita, P.; Pattanayak, S. P. *Pharmacogn. Rev.* **2011**, *5*, 41−47.
(59) Lin, C. Y.; Strom, A.; Li Kong, S.; Kietz, S.; Thomsen, J. S.; Tee, J. B.; Vega, V. B.; Miller, L. D.; Smeds, J.; Bergh, J.; Gustafsson, J. A.; Liu, E. T. *Breast Cancer Res.* **2007**, *9*, R25.
(60) Patisaul, H. B.; Jefferson, W. *Front. Neuroendocrinol.* **2010**, *31*, 400−419.
(61) Hu, K.; Jeong, J. H. *Arch. Pharmacal Res.* **2006**, *29*, 563−565.
(62) Tyagi, A. M.; Srivastava, K.; Mansoori, M. N.; Trivedi, R.; Chattopadhyay, N.; Singh, D. *PLoS One* **2012**, *7*, e44552.

DOI: 10.1021/acs.jnatprod.7b00927
J. Nat. Prod. 2018, 81, 1343−1356